Interfacial Evaluation of Flax and Hemp Fibers/Polypropylene Composites Using Micromechanical Test and Acoustic Emission

Tran Quang Son, Joung-Man Park† , Byung-Sun Hwang*

Micromechanical 시험법과 음향방출을 이용한 Flax 와 Hemp섬유 강화된 Polypropylene 복합재료의 계면 물성 평가

트란콩손, 박종만†, 황병선*

KEY WORDS: green composites, natural fiber, interfacial evaluation, Interfacial shear strength (IFSS), fragmentation test, acoustic emission.

ABSTRACT

Interfacial evaluation of various combinations of both Flax and Hemp fibers/polypropylene were performed by using micromechanical test and nondestructive acoustic emission (AE). It can be because interfacial adhesion between the natural fiber surface and matrix plays an important role in controlling the overall mechanical properties of polymer composite materials by transferring the stress from the matrix to the fiber. It is necessary to characterize the interphase and the level of adhesion to understand the performance of the composites properly. Microfailure mechanism of single Flax fiber bundles were investigated using the combination of single fiber tensile test and nondestructive acoustic emission. Microfailure modes of the different natural fiber/polypropylene systems were observed using optical microscope and determined indirectly by AE and their FFT analysis.

Nomenclature

τ	: Interfacial shear strength (IFSS)
F	: Debonding force
P	: Low population portion
q	: High population portion
D	: Fiber diameter
l	: Embedded length:
α	: Scale parameter
β	: Shape parameter
SD	: Standard deviation
COV	: Coefficient of variation

School of Materials Science and Engineering,
Engineering Research Institute,
Gyeongsang National University
*Composite Materials Laboratory
Korea Institute of Machinery and Materials
†To whom correspondence should be addressed.

1. INTRODUCTION

Over the past two decades plant fibers have been receiving considerable attention as a substitute for synthetic fiber reinforcement such as glass in plastics. The advantages of plant fibers are low cost, low density, acceptable specific strength, and good thermal insulation properties, reduced tool wear, reduced dermal and respiratory irritation, renewable resource and recycling possible without affecting the environment, and together with biodegradable ability [1-4]. However, in natural the plant fibers exhibit a high hydrophilic property as they are composed of lingo-cellulose, which contain strongly polarized hydroxyl groups. These fibers are inherently incompatible with hydrophobic thermalplastics such as polypropylene and especially for poor interfacial adhesion between the hydrophilic natural fibers and resin matrixes [4]. The final mechanical behavior of a composite material depends to a great extent on the adhesion between the reinforcing fiber and the

surrounding matrix. So it is necessary to extensively evaluate the interfacial shear strength (IFSS) between the natural fiber and resin matrix which is one of the most important factors in controlling the overall properties of the composites such as off-axis strength, fracture toughness, environmental stabilities by transferring the load from matrix material through the interphase onto the fibers which have the high tensile strength. There are several methods available to quantify the interfacial adhesion in composite materials [5,6]. In the case of single fiber composite model, some techniques such as the micro-pullout test, the single fiber fragmentation test were used.

2. EXPERIMENTAL

2.1. Materials

Hemp and Flax fibers (Carol Leigh's Hillcreek Fiber Studio, U.S.A.) were used as reinforcing fibers for green composites. Polypropylene (PP) was used as thermoplastic matrix material (Polymirae Inc., Korea).

2.2. Methodologies

2.2.1. Measurement of single fiber tensile strength: Flax and Hemp fibers were fixed on the paper frame using Kapton tape with various gauge lengths, 5, 10, 20, and 50 mm, respectively. The tensile strength of biodegradable fibers with the various gauge lengths were obtained using about sixty specimens for meaningful value and statistically analyzed using both uni- and bimodal Weibull distributions. The fiber failure process of the unimodal cumulative Weibull distribution function based on one type of defect is

$$F(t) = 1 - \exp\left[-\left(\frac{t}{\alpha}\right)^{\beta}\right] \qquad (1)$$

Where α and β are the shape and scale parameters, respectively. The cumulative bimodal Weibull distribution function based on the presence of two kinds of defect is described as

$$F(t) = 1 - \left\{ p \exp\left[-\left(\frac{t}{\alpha_1}\right)^{\beta_1}\right] + q \exp\left[-\left(\frac{t}{\alpha_2}\right)^{\beta_2}\right]\right\}$$
$$p + q = 1 \qquad (2)$$

Where p and q are the portions of low and high strength population, and β_1, α_1, β_2, and α_2 are the shape and scale parameters for the low and high strength portions, respectively.

2.2.2. Specimen Preparation and IFSS Measurement: The natural fibers were fixed with regularly separated distance in a steel frame. Microdroplets of polypropylene matrix were formed on each the natural fiber using a tip pin. A microdroplet specimen was fixed by the microvice using a specially-designed micrometer. The IFSS was calculated from the measured pullout force, F using the following equation,

$$\tau = \frac{F}{\pi D_f L} \qquad (3)$$

Where D_f and L are fiber diameter and fiber embedded length in the matrix, respectively.

3. RESULTS AND DISCUSSION

3.1. Morphology and structure of natural fibers: Figure 1 shows morphology and structure of natural microfibril is composed of several high oriented elementary fibers embedded by some matrix materials such as lignin, hemicelluloses, water, and extractives. The elementary fiber is based on cellular material, which is defined as a linear, crystalline polymer composed of (1-4) linked β-D-glucopyranose and can respond to high stress. Whereas hemicelluloses, waxes, lignin have low tensile strength and make poor adhesion between the fiber surface and matrix materials due to high hydrophilic property. Figure 2 shows morphology in diameter direction, for the natural fibers its diameter is not circular.

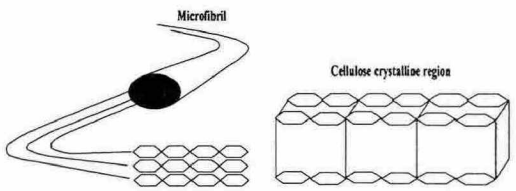

Figure 1. Morphology and structure of natural fiber.

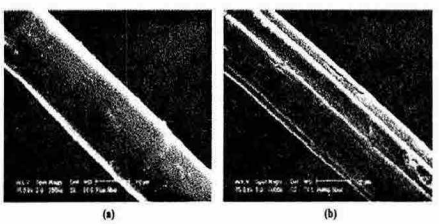

Figure 2. (a)Flax fiber, (b) Hemp fiber.

3.3. Elementary fiber modulus and strength:

Young's modulus and strength of elementary Hemp and Flax fibers were determined by SFT test. Young's modulus exhibits a large scatter with the diameters as shown in Figure 3. It may be because the chemical composition and the structure of the natural fibers depend on many factors. So far the different fibers have the different density. The fiber strength of each fiber was measured for 60 untreated fiber specimens with gauge length of 20 mm and the average diameter of 10.85 μm for Hemp fiber of 10.23 μm for Flax fiber. The obtained parameter values are given in Table 1. In here the tensile strength of both fibers is slightly different. It is consistent with their chemical structures.

Table 1. Mechanical properties of Flax and Hemp fiber

Gauge length (mm)	Diameter (μm)	Tensile Strength (MPa)	Elongation (%)	COV[b] (%)	α[c]	β[d]
Hemp	10.86 (1.6)[a]	2140 (504)	1.8 (0.7)	23.5	2342	4.6
Flax	10.23 (1.1)	2396 (652)	2.1 (0.5)	27.2	2560	4.7

a Standard deviation (SD)
b Coefficient of variation (COV) for tensile strength = SD/mean*100
c Scale parameter for fiber strength
d Shape parameter for fiber strength

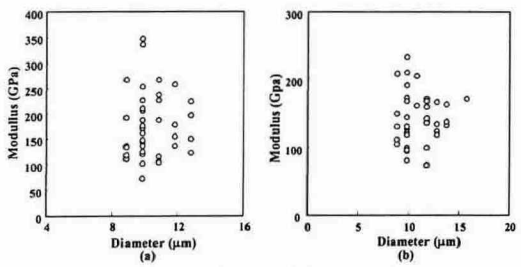

Figure 3. The natural fiber modulus as a function of fiber diameter

3.4. Analysis of strength distribution: From the tensile strength tests of both Hemp and Flax fibers, the strength distributions of the different fibers were analyzed by uni- and bimodal Weibull distributions. Figure 4 shows the cumulative strength distribution of Flax and Hemp fibers at the gauge length of 20 mm. The experimental strength data were estimated from F(N) = i/(N+1), in here N is the total number of samples tested and 'i' is the ith number in ascendingly ordered strength data. It is easy noted that for both Flax and Hemp fiber the bimodal distribution curves is more fitting with measured data than the unimodal distribution curves, which means that the natural fibers inherently contain at least two defects inside of their structures.

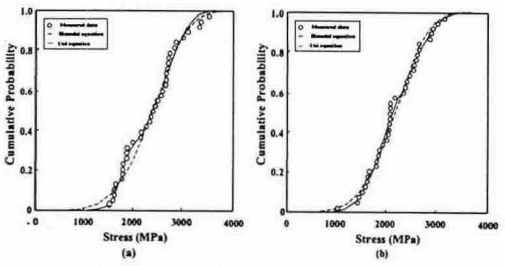

Figure 4. Unimodal and bimodal weibull distribution curves for the strength: (a)Flax fiber; (b) Hemp fiber.

3.5. Microdroplet test: Figure 5 shows the plots of debonding force versus the embedded area for various natural fibers/polypropylene composites in microdroplet test. The Critical embedded area means the intimate contacting area between fiber and matrix. In here the critical embedded area was used instead of critical embedded length due to the different diameter for both fibers. The critical embedded area was obtained by intersection of two linear regression lines: one is the fiber pullout linear regression line, whereas another is the fiber fracture linear regression line. The critical embedded area can be correlated to IFSS values. The critical embedded area of Flax fiber system is narrower than that of Hemp fiber case. The narrower the critical embedded area, the higher the IFSS value. It is consistent with their structures and chemical composition, Hemp fiber contains some more chemical compositions such as hemi-celluloses, lignin, and waxes than Ramie fiber. These chemical agents make adhesion between the fiber surface and matrix material poor due to their hydrophilic property.

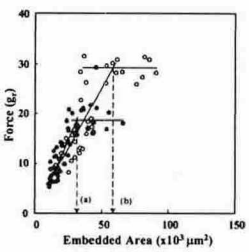

Figure 5. Debonding force – embedded area curves: (a) Flax fiber; (b) Hemp fiber.

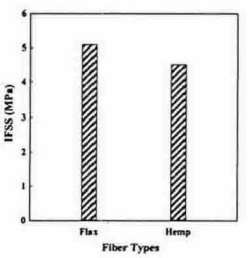

Figure 6. IFSS of different natural fiber/PP composites.

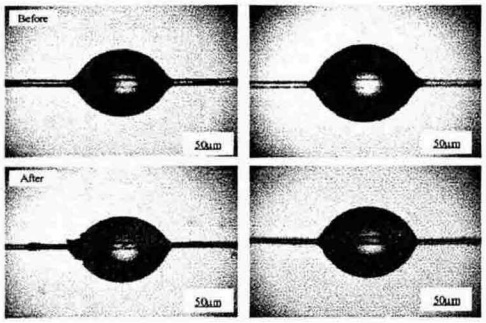

(a) (b)

Figure 7. Typical microfailure modes of the natural fiber/polypropylene: (a) hemp fiber; (b) Flax fiber.

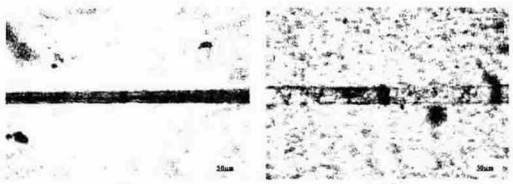

(a) (b)

Figure 8. *Typical microfailure modes of the natural fiber/polypropylene: (a) Flax fiber; (b) Hemp fiber.*

3.6. IFFS measurements: Figure 6. Shows the IFSS of four untreated natural fiber/polypropylene systems calculated for each sample according to the equation (3) and then the IFSS of each system was determined by simple averaging. The IFSS of Kenaf fiber/polypropylene is the lowest, whereas the IFSS of the other systems were slightly different. It is consistent with the structures and their chemical composition. Figure 7 shows the photographs of the typical microfailure modes of Flax and Hemp fibers/polypropylene systems, the microdroplets appeared matrix crack modes and thus pulled out shape due to less strong interfacial adhesion. Figure 8 shows the microfailure modes under tension for both Flax and Hemp fibers/polypropylene systems.

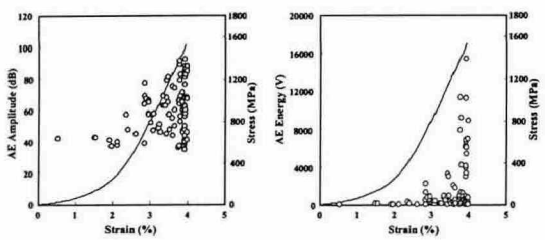

Figure 9. AE amplitude and AE energy of single Flax fiber bundle.

For both the systems, the microfailure modes include debonding between the fiber surface and matrix material, cracks of elementary fibers, and fracture of elementary and fibril fibers.

3.7. Microfailure mechanism of single fiber bundle

The AE amplitude and AE energy values in Figure 9 already indicated that low amplitudes and AE energies appear in the initial fracture, whereas high AE amplitude and energy signals were emitted close to the final fracture of the fibers.

CONCLUSION

Interfacial evaluation of Flax and Hemp fibers/polypropylene composites was performed using microdroplet test. IFSS of Kenaf fiber/polypropylene system is significantly lower than that of the other natural fiber/polypropylene systems, it may be because the difference of their structure and chemical composition. Mechanical properties of Flax and Hemp fibers such the tensile strength, tensile modulus, and the elongation at gauge length of 20 mm and given diameters were investigated using single fiber tensile test and statistically analyzed using both uni- and bimodal Weibull distributions. From the analytical results showed that the bimodal Weibull distribution was more fitting with measured data than the unimodal distribution. The microfailure modes of various Flax and Hemp fibers/polypropylene systems were investigated for both the microdroplet specimens and the dogbone shaped specimens under tension. The microfailure mechanism of the single Flax fiber bundle was clarified using nondestructive acoustic emission technique.

ACKNOWLEDGMENT: this research was supported by MOST-MOCIE of Korea under contract M10436010010-04L3601-01-000.

REFERENCES

(1) M. Brahmakumar, C. Pavithran, R.M. Pillai, *Compos Sci Technol,* 65, 1999, pp 309-320.

(2) A. Valadez-Gonzalez, J.M. Cervantes-Uc, R.Olayo, P. J. Herrera-Franco, *Compos. Part B*, 30, 1999, pp 309-320.

(3) G. Romhany, J. Karger-Kocsis, T. Czigany, *J Appl Polym Sci,* 90, 2003, pp 3638-3645.

(4) N.E. Zafeiropoulos, C.A. Baillie, J.M. Hodgkinson, *Compos. Part A,* 33, 2002, pp 1185-1190.

(5) J.M. Park, D.S. Kim, S.R. Kim, *Compos Sci Technol,* 64, 2004, pp 847-860.

(6) J.M. Park, D.S. Kim, S.R. Kim, *J Colloid Interf Sci,* 264, 2003, pp 431-445.